



Bacterial Community Assembly, Succession, and Metabolic Function during Outdoor Cultivation of *Microchloropsis salina*

 Megan M. Morris,^a Jeffrey A. Kimbrel,^a Haifeng Geng,^b Mary Bao Tran-Gyamfi,^c Eizadora T. Yu,^{b,d,*}  Kenneth L. Sale,^c Todd W. Lane,^b  Xavier Mayali^a

^aPhysical and Life Sciences Directorate, Lawrence Livermore National Laboratory, Livermore, California, USA

^bDepartment of Systems Biology, Sandia National Laboratories, Livermore, California, USA

^cDepartment of Computational Biology and Biophysics, Sandia National Laboratories, Livermore, California, USA

^dThe Marine Science Institute, University of the Philippines Diliman, Quezon City, Philippines

ABSTRACT Outdoor cultivation of microalgae has promising potential for renewable bioenergy, but there is a knowledge gap on the structure and function of the algal microbiome that coinhabits these ecosystems. Here, we describe the assembly mechanisms, taxonomic structure, and metabolic potential of bacteria associated with *Microchloropsis salina* cultivated outdoors. Open mesocosms were inoculated with algal cultures that were either free of bacteria or coinoculated with one of two different strains of alga-associated bacteria and were sampled across five time points taken over multiple harvesting rounds of a 40-day experiment. Using quantitative analyses of metagenome-assembled genomes (MAGs), we tracked bacterial community compositional abundance and taxon-specific functional capacity involved in algal-bacterial interactions. One of the inoculated bacteria (*Alteromonas* sp.) persisted and dispersed across mesocosms, whereas the other inoculated strain (*Phaeobacter gallaeciensis*) disappeared by day 17 while a taxonomically similar but functionally distinct *Phaeobacter* strain became established. The inoculated strains were less abundant than 6 numerically dominant newly recruited taxa with functional capacities for mutualistic or saprophytic lifestyles, suggesting a generalist approach to persistence. This includes a highly abundant unclassified *Rhodobacteraceae* species that fluctuated between 25% and 77% of the total community. Overall, we did not find evidence for priority effects exerted by the distinct inoculum conditions; all mesocosms converged with similar microbial community compositions by the end of the experiment. Instead, we infer that the 15 total populations were retained due to host selection, as they showed high metabolic potential for algal-bacterial interactions such as recycling alga-produced carbon and nitrogen and production of vitamins and secondary metabolites associated with algal growth and senescence, including B vitamins, tropodithetic acid, and roseobactin.

IMPORTANCE Bacteria proliferate in nutrient-rich aquatic environments, including engineered algal biofuel systems, where they remineralize photosynthates, exchange secondary metabolites with algae, and can influence system output of biomass or oil. Despite this, knowledge on the microbial ecology of algal cultivation systems is lacking, and the subject is worthy of investigation. Here, we used metagenomics to characterize the metabolic capacities of the predominant bacteria associated with the biofuel-relevant microalga *Microchloropsis salina* and to predict testable metabolic interactions between algae and manipulated communities of bacteria. We identified a previously undescribed and uncultivated organism that dominated the community. Collectively, the microbial community may interact with the alga in cultivation via exchange of secondary metabolites which could affect algal success, which we demonstrate as a possible outcome from controlled experiments with metabolically analogous isolates. These findings address the scalability of lab-based algal-bacterial interactions through to cultivation systems and more broadly provide a framework for empirical testing of genome-based metabolic predictions.

Editor Hideyuki Tamaki, National Institute of Advanced Industrial Science and Technology

This is a work of the U.S. Government and is not subject to copyright protection in the United States. Foreign copyrights may apply.

Address correspondence to Megan M. Morris, morris81@llnl.gov.

*Present address: Eizadora T. Yu, Institute of Chemistry, National Science Complex, University of the Philippines, Diliman Quezon City, Philippines.

The authors declare no conflict of interest.

Received 16 May 2022

Accepted 3 June 2022

Published 22 June 2022

KEYWORDS algal-bacterial interactions, metagenome-assembled genomes, community assembly, *Rhodobacteraceae*, *Microchloropsis*

Photosynthetic eukaryotes, known as algae, coexist with and are shaped by heterotrophic synergistic bacteria (the algal microbiome) in all aquatic environments (1, 2). Heterotrophic bacteria incorporate (3), remineralize, and decompose alga-derived organic carbon and nitrogen (4), significantly impacting resource availability and nutrient pools on local to global biogeochemical scales (5, 6). Bacteria also have the capacity to affect algal growth and survival through complex secondary metabolic interactions. Mutualistic bacteria enhance algal success, producing exogenous vitamins (7–9), cross-kingdom signaling compounds and phytohormones (10, 11), and antimicrobial compounds that stimulate algal growth (12), influence reproductive events (13), and protect against invading antagonists (14), all of which enhance algal productivity. On the flip side, bacterial antagonists inhibit algal productivity (15) through nutrient competition under oligotrophic conditions, production of algicidal compounds (16, 17), or the physical lysing of algal cells (18, 19). These dichotomous interactions, bounded between mutualistic and antagonistic relationships, are often context dependent based on the taxonomic identity and functional capacity of each partner, resulting in a spectrum of physiological outcomes for the algae. Therefore, we must consider the inevitable influence of bacteria on algal productivity, uniquely for engineered biofuel systems, where yield dictates economic impact.

Large-scale cultivation of both macro- and microalgae is gaining interest as a renewable, economically viable energy source (20). Algal biofuel applications are engineered to maximize yield, and due to the nature of the system where cultures are produced en masse, even incremental increases in algal productivity on a local pond level can have compounding effects on a system-wide scale (21). To increase algal productivity, resilience, and overall biomass yield, altering the bacterial community could be leveraged, with the goal of establishing a beneficial partnership in the algal-bacterial coculture (22–24). However, for algal biofuels to remain sustainable, productive, and high throughput while minimizing operations cost, commercial applications are gravitating toward open outdoor systems with less controlled conditions (25), sacrificing the sterility of axenic (bacteria-free) algal cultures (26). Therefore, if mutualistic bacteria are to be used in coculture with algae for applied biofuels, we should fully understand not only how they interact with algae but also how they interact with other bacterial consortia invariably introduced during outdoor cultivation.

The potential to more fully encapsulate algal-bacterial interactions across spatial and temporal scales (27) is greater than ever in part due to advancements in molecular characterization of bacterial community taxonomic structure (28) and metabolic function (29, 30). The mechanisms and processes that drive community assembly are widely studied in ecology (31) yet are underrepresented for algal systems biology, in particular how bacterial community assembly impacts system-level dynamics (32, 33). Of the few studies which have examined this topic, those that utilize a reductionist approach in highly controlled synthetic systems show that bacterial community assembly is predictable and shaped by specific algal exometabolites (34, 35). While the primary structuring force for alga-associated bacteria is metabolite production driven by algal host identity (36–39), in more complex systems akin to algal biofuel cultivation systems, bacterial community composition is greatly influenced by initial inoculum and culture conditions (32), as the type and availability of metabolites exchanged with and among bacteria will affect bacterial succession and persistence (40–42). It is important to predict how not only community composition but also, more importantly, metabolic function is shaped in algal cultivation systems, as alternate community capacities will likely influence algal productivity.

In this study, through molecular characterization of empirical ecological experiments, we follow the trajectory of bacterial community assembly in an open microalgal cultivation system. We describe the taxonomic structure, metabolic potential, and biogeochemical capabilities of both inoculated and recruited bacteria via comparative genomics of metagenome-assembled genomes (MAGs), inferring the ecological roles of bacteria that become

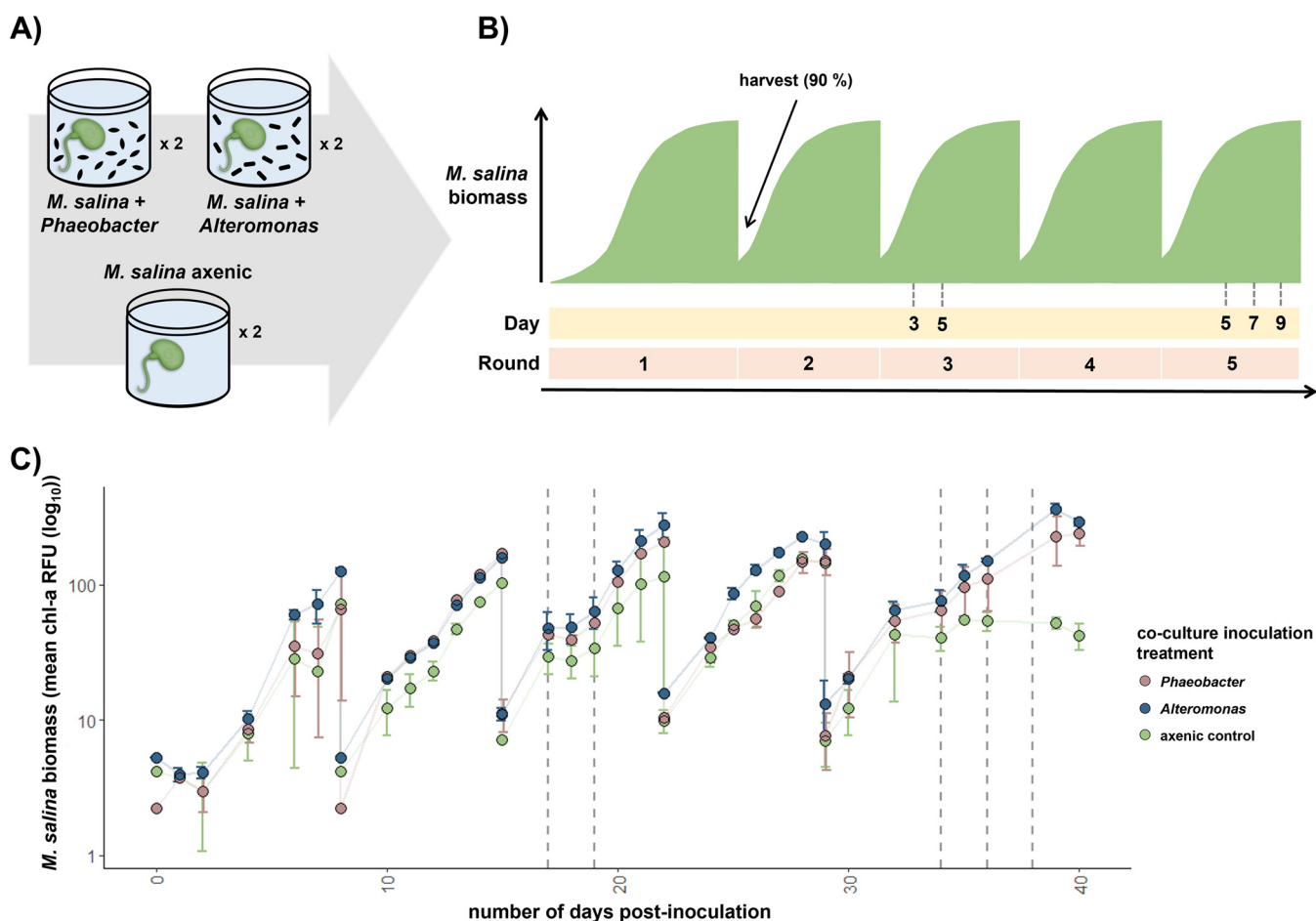


FIG 1 Experimental design of algal-bacterial coculture mesocosms and resulting algal biomass over time. (A) Duplicate 16-L algal mesocosms of *M. salina* inoculated with either *Phaeobacter gallaeciensis* BS107 or *Alteromonas* sp. I10 or left axenic at day 0. (B) Mesocosms were left open to bacterial dispersal and maintained for 40 days, with 5 rounds of harvest in which 90% of algal biomass was removed and 10% of biomass was retained into the subsequent round. Dashed lines indicate when DNA for metagenomes was collected. (C) *M. salina* biomass measured over time by chlorophyll *a* fluorescence (log₁₀ scale). Colors indicate initial inoculation treatment: *Phaeobacter* (red), *Alteromonas* (blue), and axenic culture (green). Points represent the mean result of each treatment at each time point sampled, with error bars indicating standard deviation. Dashed lines correspond with metagenomic sampling time points (cultivation round 3: days 17 and 19; round 5: days 34, 36, and 38).

established within an algal culture system. We investigated whether distinct inoculations of bacteria may exhibit priority effects that divergently affect community development over time and whether these system dynamics may affect resulting algal success. Based on the molecular characterizations of the cultivation system, we predicted metabolic interactions between the alga and the bacteria, which we subsequently tested under controlled laboratory cocultivation with metabolically analogous strains. This study not only characterizes the composition, metabolic capacity, and ecological roles of bacteria that are recruited within a biotechnologically relevant algal cultivation system but also more broadly assesses the scalability of laboratory-defined algal-bacterial interactions in complex systems and is relevant to future studies seeking to engineer bacterial communities that enhance algal biofuel productivity.

RESULTS

Fifteen numerically dominant bacterial taxa associated with outdoor *M. salina* cultures. *Microchloropsis salina* algal mesocosms were initially established with one of three inoculum treatment conditions: (i) coculture with *Phaeobacter gallaeciensis* BS107, (ii) coculture with *Alteromonas* sp. strain I10, or (iii) axenic culture (Fig. 1A). *M. salina* biomass did not vary by bacterial inoculation treatment except for the final time points, when both mesocosms originally inoculated with the axenic culture had lower biomass than the other

four mesocosms (Fig. 1C). While we were unable to attribute the differences in biomass to the presence of a specific bacterial taxon, we subsequently leveraged clues from bacterial community structure and metabolic capacity to infer system dynamics.

We identified *M. salina*-associated bacterial taxa and their corresponding metabolic capacities with metagenome-assembled genomes (MAGs) cross-assembled from 30 samples taken from the 6 mesocosms at 5 distinct time points (days 17 and 19 from round 3; days 24, 36, and 38 from round 5) (Fig. 1B; see Table S1 in the supplemental material). The MAGs were representative of the vast majority of bacterial reads, with 89.6% of reads mapped to 15 high-quality curated MAGs (Table S2 and Text S1). The 15 bacterial MAGs spanned 7 families, with 10 classified at the genus level (*Algoriphagus*, *Alteromonas*, *Erythrobacter*, *Flavobacterium*, *Marinobacter*, *Marinoscillum*, *Methylophaga*, *Phaeobacter*, *Pseudophaeobacter*, *Roseibaca*) and five unclassified at the genus level or higher (Fig. 2; Table S2).

Retention of primary inoculated strains varied temporally and by treatment.

Since four of the six mesocosms were initially inoculated with alga-associated bacterial strains of the genera *Alteromonas* and *Phaeobacter*, we first searched the metagenomes for these organisms. We recovered one nearly complete MAG for each of these two genera. The MAG corresponding to *Phaeobacter gallaeciensis* BS107 (named MSM14), with closest neighbor GTDB lineage as *Phaeobacter gallaeciensis*, exhibited 89.71% average pairwise nucleotide identity (ANI) compared to the *P. gallaeciensis* BS107 reference genome. The MSM14 genome was 78.07% complete, with 1.91% contamination and 59.1% GC content. These data suggest that the *Phaeobacter* strain initially added to the mesocosms had disappeared within the first 17 days and was replaced with a related yet distinct *Phaeobacter* sp. (MSM14) that was recruited to all 6 mesocosms and persisted at low to moderate abundances (Table S7A). On the other hand, the MAG corresponding to *Alteromonas* sp. I10 (MSM1), with closest neighbor GTDB lineage as *Alteromonas macleodii*, exhibited 99.99% ANI compared to the *Alteromonas* sp. I10 reference genome. The MSM1 genome was 100% complete, with 0.36% contamination and 44.6% GC content (Table S2). The presence of *Alteromonas macleodii* (MSM1) in its respective treatment mesocosms, and its dispersal to neighboring mesocosms, varied over time (Fig. 2; Table S7A and Fig. S1). This shows that the initially added *Alteromonas* remained present throughout the two mesocosms where it was inoculated and had dispersed to the other four mesocosms as well.

Bacterial recruitment was taxon specific, and prevalence varied temporally. In addition to the two bacterial strains initially inoculated within respective treatments (one remaining throughout and the other showing lack of establishment/persistence), 14 other bacterial taxa were recruited to the 6 mesocosms at high enough abundances to recover medium- to high-quality MAGs (Tables S2 and S7A). Between 7 and 13 taxa cooccurred in any given sample. In order to estimate the contribution of each taxon within the collective community structure, we quantified the abundance of each bacterial MAG with a fold coverage metric (Table S7B). Fold coverage was also transformed relative to all MAGs within each sample, referred to hereafter as “relative coverage”, to appropriately compare MAG predominance across treatments and over time (Table S7C). One MAG (unclassified *Rhodobacteraceae* MSM9) showed remarkably high relative coverage across all samples, as high as ~77% in one sample (~223-fold coverage), and on average representing ~50% of the MAG community. An additional 5 MAGs had intermediate abundance, with their genomes covering at least 1.6-fold in any given sample (Fig. 2G; Fig. S1). The remaining 9 bacterial MAGs, including the inoculated *Alteromonas* sp., were less predominant system-wide and encompassed <1% of the bacterial community (Fig. 2H; Tables S7B and S7C).

We aimed to test whether MAG community taxonomic composition varied by inoculation treatment and temporally throughout the algal cultivation cycles and used relative coverage for this comparison. While mesocosms were initially inoculated with specific bacterial strain starting conditions (*Phaeobacter*, *Alteromonas*, axenic control), all taxa were shared among the treatment mesocosms by the midpoint of the experiment, as the overall MAG composition did not significantly vary with inoculation treatment (Bray-Curtis dissimilarity, permutational multivariate analysis of variance [PERMANOVA]: $r^2 = 0.083$, $P = 0.082$). The relative coverage (or abundance) of bacteria did however vary over time

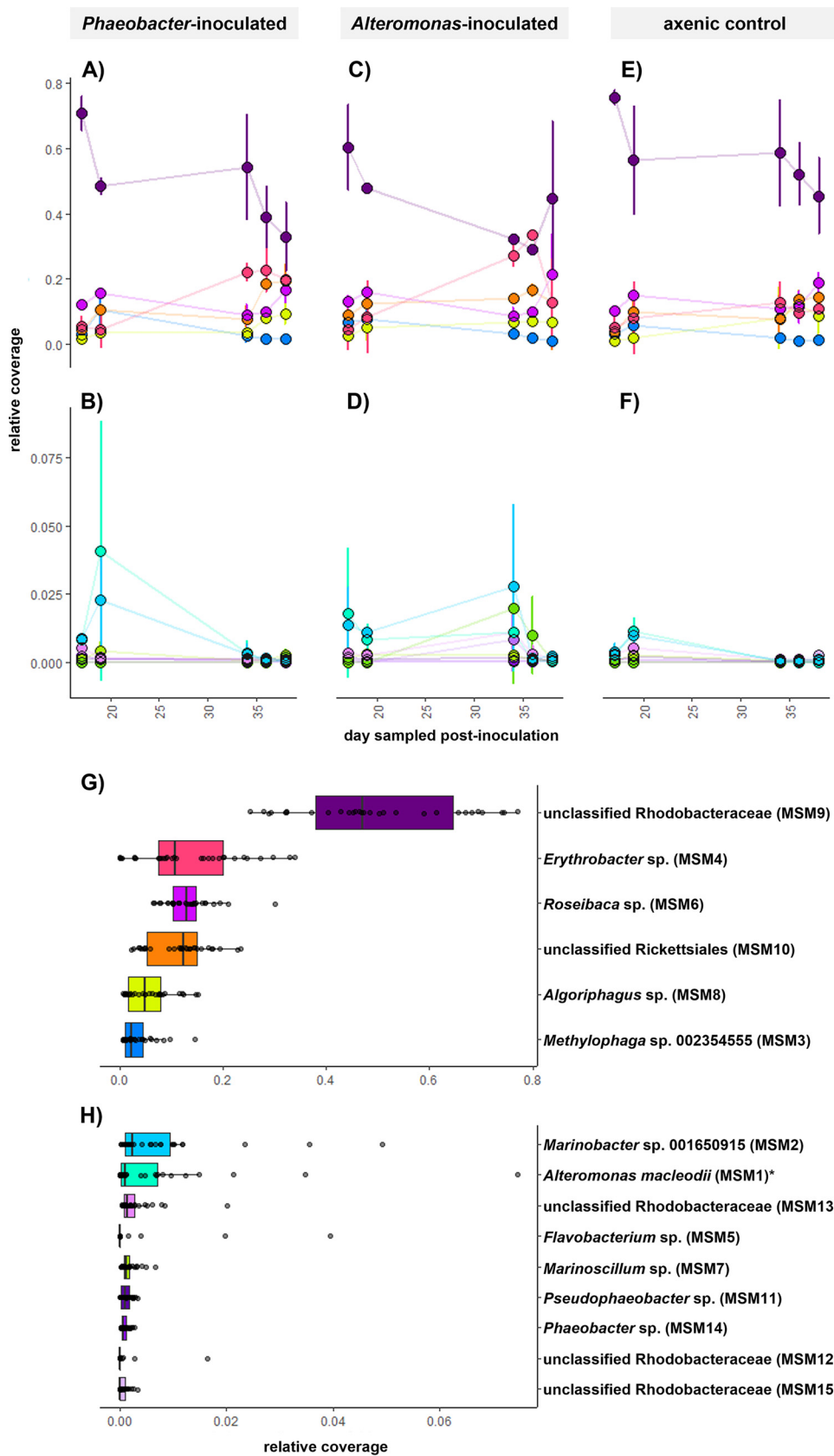


FIG 2 Estimated relative abundance of *M. salina*-associated bacteria over time. Abundance of each of the 15 bacterial taxa inoculated or recruited within the *M. salina* algal cultivation system was estimated using the (Continued on next page)

(PERMANOVA: $r^2 = 0.481$, $P < 0.001$) (Fig. 2; Fig. S1), with three MAGs contributing the greatest differentiation (SIMPER analysis): unclassified *Rhodobacteraceae* (MSM9) (31.85 to 37.38% dissimilarity contribution), *Erythrobacter* sp. (MSM4) (17.81 to 23.68% dissimilarity contribution), and unclassified Rickettsiales (MSM10) (15.03 to 19.96% dissimilarity contribution). Of those three bacterial taxa, *Erythrobacter* sp. (MSM4) varied in abundance across treatment mesocosms just 3 days prior (day 36) to divergence in mesocosm productivity (day 39). Early in the cultivation experiment, this taxon was similarly represented (~10% relative coverage) across the mesocosms (days 17 and 19). It subsequently increased in abundance through day 36 in the mesocosms that produced higher biomass (*Alteromonas* inoculated, $33.47\% \pm 0.79\%$ relative coverage; *Phaeobacter* inoculated, $22.63\% \pm 6.65\%$ relative coverage) but remained at lower abundances in the reduced-biomass mesocosms (control, $9.66\% \pm 0.60\%$ relative coverage) (Fig. 1C; Fig. S1). This was the only taxon whose abundance appeared to correlate with algal mesocosm biomass.

MAG population-level variation via SNP detection. The high coverage of the unclassified *Rhodobacteraceae* (MSM9) MAG from all 30 metagenomes allowed us to examine genome heterogeneity across samples, both over time and across inoculation treatment. Since lower sequencing coverage may lead to false-positive detection of single nucleotide polymorphisms (SNPs), we did not perform this analysis on the remaining 14 MAGs. MSM9 represented a very high proportion of the total bacterial community and thus had a high fold coverage overall. As such, our analysis could determine if there were multiple recruitment events of this strain into the mesocosms, with either different strains being recruited to different mesocosms or new strains displacing old strains over time. Our analysis detected just 9 potential SNPs out of the entire 3.76-Mb genome (<0.001% variation). Further, these 6 potential SNPs were distributed seemingly randomly across mesocosms, meaning that there was no discernible SNP pattern by treatment or over time. Due to the lack of sampling earlier in the experiment, it is unknown what the exact order of arrival was of this particular bacterial strain.

***M. salina*-associated heterotrophic aquatic bacteria capable of aerobic C and N remineralization.** Dense algal cultures and natural blooms are overly saturated with oxygen, at least during the day, due to photosynthesis, and algal cells are known to release dissolved organic carbon (DOC), so we expected the *M. salina*-associated bacteria to exhibit metabolic genes for survival under these conditions. We first examined the general biogeochemical capacity based on marker genes for carbon (C) and nitrogen (N) cycling (43). Overall, the *M. salina* bacterial community harbored pathways for common aerobic carbon cycling processes, such as aerobic C respiration, and processes less expected to be dominant in algal blooms, such as CO oxidation and aerobic C fixation. Examination of these patterns at the taxon level showed that the different bacterial taxa varied in their metabolic capacity for C utilization and remineralization. For example, while most bacteria ($n = 13$ MAGs) contained all required marker genes for aerobic respiration, *Pseudophaeobacter* sp. (MSM11) and *Methylophaga* sp. (MSM3) lacked 50% and 100% of the required genes for this process, respectively. A smaller subset of bacteria ($n = 6$ MAGs) were capable of CO oxidation, including *P. gallaeciensis*, *Pseudophaeobacter* sp.

FIG 2 Legend (Continued)

mean of the median fold coverage of metagenomic contigs from each sample ($n = 30$ total) against the comprehensive metagenome-assembled genome (MAG) and was normalized within each sample by transformation to a relative proportion, referred to as the "relative coverage." (A to F) Facets represent MAG coverage averaged across duplicate mesocosms \pm standard deviation for each inoculation treatment, i.e., *Phaeobacter* inoculated (A and B), *Alteromonas* inoculated (C and D), and uninoculated axenic control (E and F) with 5 time points sampled for each treatment (round 3: days 17 and 19; round 5: days 34, 36, and 38). Higher-abundance taxa are shown in the upper row (A, C, E, and G), and lower-abundance taxa are represented in the bottom row (B, D, F, and H). (G and H) Box plots show distribution of MAG relative coverage system-wide for all samples, sorted in decreasing order of abundance. Colors represent MAG taxonomic groups as follows: class Alphaproteobacteria in warm colors, including *Rhodobacteraceae* (purples) (MSM6, MSM9, MSM11, MSM12, MSM13, MSM14, MSM15), *Sphingomonadaceae* (red) (MSM4), and unclassified Rickettsiales (orange) (MSM10); class Bacteroidia in greens, including *Cyclobacteriaceae* (MSM7, MSM8) and *Flavobacteriaceae* (MSM5); and class Gammaproteobacteria in blues, including *Alteromonadaceae* (MSM1), *Methylophagaceae* (MSM3), and *Oleiphilaceae* (MSM2). An asterisk indicates the MAG recovered from one of two inoculated strains.

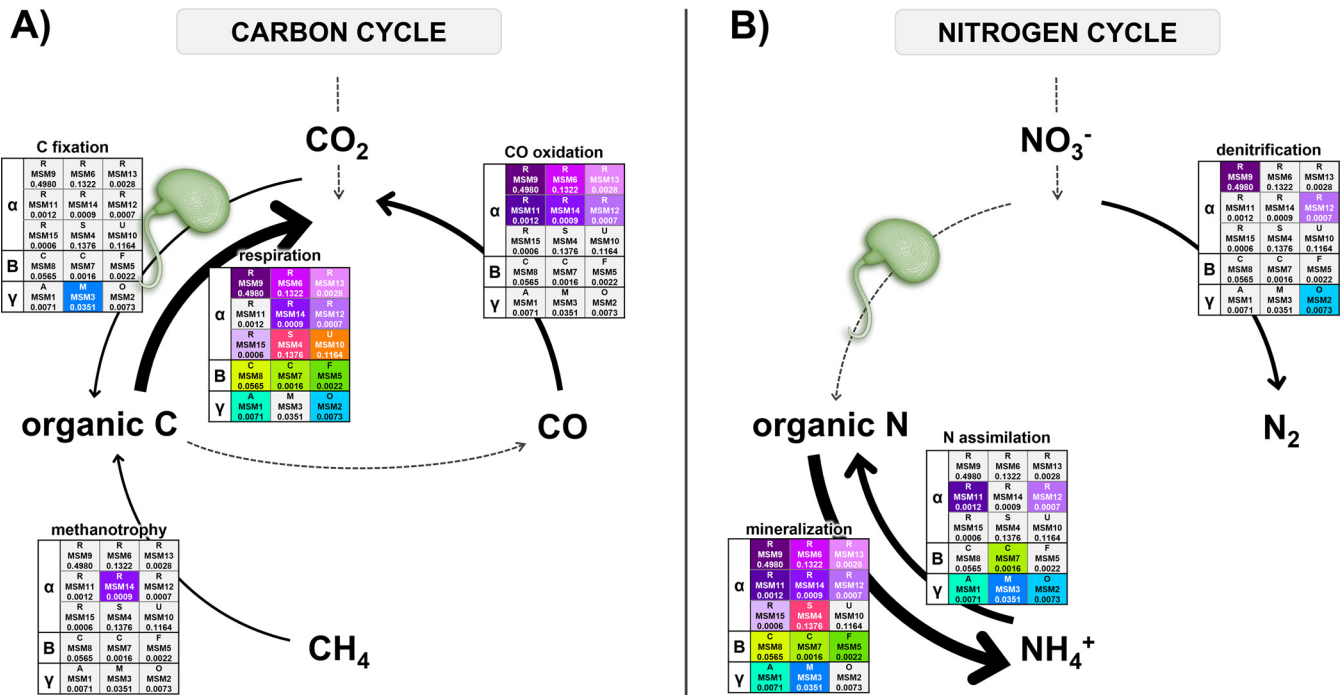


FIG 3 Biogeochemical capabilities of *M. salina*-associated bacteria. The bacterial biogeochemical capacity was determined by pathway marker gene presence (>75%). (A) Bacterial capabilities for specific metabolic pathways within the carbon cycle, including carbon fixation, respiration, methanotrophy, and carbon monoxide oxidation. (B) Bacterial metabolic capacities for steps of the nitrogen cycle, including assimilation, mineralization, and denitrification. MAGs are grouped by their respective taxonomic classifications by class and by family within each class grouping (α = Alphaproteobacteria: R = *Rhodobacteraceae* [purples], S = *Sphingomonadaceae* [red], U = unclassified Rickettsiales [orange]; B = Bacteroidia: C = *Cyclobacteriaceae* [yellow], F = *Flavobacteriaceae* [greens]; γ = Gammaproteobacteria [blues]: A = *Alteromonadaceae*, M = *Methylophagaceae*, O = *Oleiphilaceae*). Relative coverage averaged system-wide ($n = 30$ samples) is indicated for each MAG. Arrows show flow of C and N via bacterial metabolism, weighted for thickness based on the number of MAGs capable of that specific pathway. Dashed gray arrows indicate input or conversion from nonbacterial processes.

(MSM11), *Roseibaca* sp., and three unclassified *Rhodobacteraceae* members (MSM9, MSM12, MSM13). The capability for aerobic C fixation was restricted to just one bacterium, *Methylophaga* sp., which appears to be an obligate single-carbon utilizer, able to fix C with the phosphoribulokinase (PRK) and ribulose-bisphosphate carboxylase (*rbcS*) genes. One bacterium, *Phaeobacter* sp. (MSM14) may be capable of metabolizing methane via methanotrophy (Fig. 3). All bacterial taxa lacked the full pathways for anaerobic C cycling, such as fermentation, anaerobic C fixation, and methanogenesis (Table S3). However, four of the bacteria were predicted to be capable of photoheterotrophy, including *Erythrobacter* sp. (MSM4), *Roseibaca* sp. (MSM6), and two unclassified *Rhodobacteraceae* members (MSM12, MSM13), which contained 76.92%, 94.23%, 84.62%, and 92.31% of the 52 PGC (photosynthetic gene cluster) gene orthologs, respectively. Bacteria which were not predicted to be photoheterotrophs contained between 7.69% and 69.23% of the PGC genes (Table S4).

With respect to the N cycle, 3 of the 7 primary reactions were represented by *M. salina*-associated bacteria: mineralization, N assimilation, and denitrification. Mineralization of N was the most common pathway among bacteria, with the exception of *Marinobacter* sp. (MSM2) and the unclassified Rickettsiales (MSM10), with 13 of 15 MAGs containing all required marker genes for this process. Six taxa were capable of inorganic N assimilation, including *Alteromonas macleodii* (MSM1), *Marinobacter* sp. (MSM2), *Methylophaga* sp. (MSM3), *Pseudophaeobacter* sp. (MSM11), *Marinoscillum* sp. (MSM7), and one of the unclassified *Rhodobacteraceae* members (MSM12). Just three bacteria were capable of denitrification: *Marinobacter* sp. (MSM2) and two unclassified *Rhodobacteraceae* members (MSM9, MSM12) (Fig. 3B). None of the bacterial taxa were predicted to be capable of ammonification, anammox, N fixation, or nitrification (Table S3).

Bacteria demonstrate metabolic capabilities for influencing algal-bacterial interaction outcomes. In addition to describing the general biogeochemical capabilities of *M. salina*-inoculated and recruited bacterial taxa, we assessed the bacterial capacity for

more specialized secondary metabolisms regarded for algal-bacterial interactions, including production of beneficial B vitamins, the antimicrobial compound tropodithietic acid (TDA), and the algicidal compound roseobacticide. Twelve of the 15 bacterial taxa were capable of production of at least one class of B vitamins, with 7 capable of B1 (thiamine) synthesis, 9 capable of B7 (biotin) synthesis, and 6 capable of B12 (cobalamin) synthesis. Of these 12 B vitamin-synthesizing bacteria, just two were predicted to synthesize all three types: *Pseudophaeobacter* sp. (MSM11) and *Methylophaga* sp. (MSM3). Neither *Algoriphagus* sp. (MSM8) nor two of the unclassified *Rhodobacteraceae* members (MSM15 and the abundant MSM9) were predicted to biosynthesize any of the B vitamins (Table S5). We also examined the biphasic symbiosis mediated by bacterial metabolism of tropones—algal growth-promoting TDA (tropodithietic acid) and algicidal roseobacticides. This complex process is driven by bacterial metabolism of the alga-derived metabolite *p*-coumaric acid (pCA), which may occur either through tolerance/transport (44) or degradation (45). Bacteria produce other required precursors/intermediates via phenylacetic acid (PAA) catabolism (46) and sulfur metabolism, and products from those aforementioned steps are collectively incorporated into a troponone backbone (47) for both TDA or roseobacticide secondary metabolites. Ten *M. salina*-associated genomes ($n = 6$ Alphaproteobacteria, $n = 3$ Gammaproteobacteria, $n = 1$ Bacteroidia) contained the genes for processing pCA, either through reactions for partial degradation to 4-hydroxybenzoate (MSM5, MSM15), full degradation through to the tricarboxylic acid (TCA) cycle (MSM9, MSM11, MSM12, MSM13, MSM14), or tolerance to pCA via phospholipid transport (MSM1, MSM3), with *Marinobacter* sp. (MSM2) capable of both degradation and tolerance. Five of these taxa plus two others (MSM6, MSM7) contained the full pathway for PAA catabolism. All MAGs were capable of metabolizing sulfur intermediates via the *cysI* or *patB* genes. Only one taxon, *Phaeobacter gallaeciensis* (MSM14), was predicted to synthesize either TDA or roseobacticide compounds via TDA, as this MAG contained the suite of genes for TDA resistance (*tdaR1* to *tdaR5*) (48) and TDA backbone biosynthesis (*tdaA* to *tdaE*) (Fig. 4; Table S6).

Based on the genomic characterizations of the *M. salina* mesocosm bacterial community, we formed predictions of algal-bacterial interactions mediated by the metabolic activity of the rest of the bacterial community and tested this through a subsequent experiment. Specifically, we hypothesized that pCA-degrading bacteria might provide a mechanism to prevent algicidal activity by roseobacticide producers. We tested this under a more controlled and simplified community than the mesocosm setup, i.e., the alga *M. salina* was cocultured with the predicted TDA/roseobacticide producer *P. gallaeciensis*, with or without a bacterial consortium of 8 bacterial strains capable of pCA degradation. While pCA is produced by microalgae, here it was added exogenously to ensure availability at standardized concentrations. Given that pCA is required for bacterial production of roseobacticides, we predicted that supplementing exogenous pCA would stimulate roseobacticide production by *P. gallaeciensis*, resulting in *M. salina* growth inhibition. On the other hand, we anticipated that the addition of pCA-degrading bacteria would reduce the availability of this precursor in the medium, slowing or preventing *P. gallaeciensis* roseobacticide production and instead potentially switching bacterial metabolism to TDA synthesis, and *M. salina* growth would not be inhibited under these conditions. The experimental results were consistent with this hypothesis. Overall, we observed that *P. gallaeciensis* reduced *M. salina* biomass in comparison to axenic algal cultures, with an additional significant reduction in biomass when exogenous pCA was available (Fig. 4A). The pCA-degrading community incapable of roseobacticide synthesis also inhibited algal growth (Fig. 4B), through an as-yet-unknown mechanism. However, the inhibitory effect was not observed when both *P. gallaeciensis* and the pCA-degrading bacterial community were combined, with algal biomass equal to or slightly enhanced over that of axenic cultures (Fig. 4C; Fig. S2).

DISCUSSION

Deterministic community assembly. The addition of mutualistic bacteria in engineered algal cultivation systems has been proposed as a potential strategy for increasing

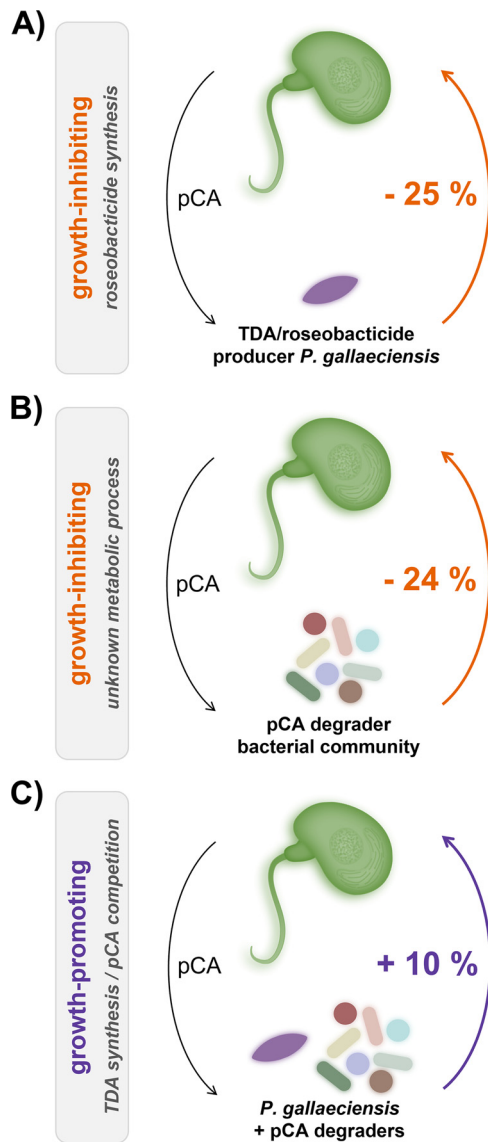


FIG 4 Biphasic outcomes of algal-bacterial interactions depending on community consortia. Here, we show a hypothetical community-based conceptual model building upon a previously described algal-bacterial biphasic interaction, supported by our genome-based predictions and experimental evidence of algal outcome under various bacterial conditions. Microalgae produce *p*-coumaric acid (pCA), which induces a metabolic response in bacteria, with some bacteria capable of tolerance via pCA degradation or conversion of pCA into algal growth-promoting (tropodithietic acid [TDA]) or growth-inhibiting (roseobacticide) compounds. (A) In the presence of exogenous pCA, the bacterium *Phaeobacter gallaeciensis*, capable of roseobacticide production, inhibited algal growth in comparison to axenic cultures free of bacterial cells. (B) A synthetic bacterial community comprised of 8 isolates, capable of pCA degradation among other metabolic characteristics, also inhibited algal growth in the presence of pCA. (C) In combination, *P. gallaeciensis* and the pCA degrader community promoted algal growth in comparison to axenic algal cultures.

biomass output (for examples, see references 22 and 24). It has been shown previously that the taxa applied in this experiment, *Phaeobacter gallaeciensis* (49, 50) and *Alteromonas* sp. (51, 52), can provide a growth-enhancing effect to *M. salina* when grown in pure coculture under certain conditions. Therefore, we hypothesized that the growth-enhancing effect of both bacterial strains would be conserved in this scaled-up cultivation system, with inoculated treatments exhibiting a higher algal biomass than that of the initially axenic control mesocosms. As the growth-enhancing effects observed in the laboratory occurred on very short time scales (days), we expected to observe that effect in this system by the end of round 1 of algal cultivation, yet we detected no discernible difference in algal

growth or biomass accumulation under the different inoculation treatments up through round 4 (Fig. 1C). Rather, a difference in algal biomass across treatments began to appear only at the very final time points, at the end of round 5 (~38 days postinoculation), when the biomass of *M. salina* in the control mesocosms was ~18% and ~14% lower than that in the *Phaeobacter*- and *Alteromonas*-inoculated treatments, respectively. While this result differed from our expectation, it might suggest that primary inoculation with a mutualist may lead to increased resilience of algae over longer-term time scales and is worth future investigation. These findings may be of relevance for applied biofuel systems, as resilience may prevent sudden crashes in algal cultivation systems that decimate biofuel output (26).

Mutualistic bacteria have also been shown to indirectly increase algal output by altering the composition of the surrounding bacterial community, for example, by excluding competitive or antagonistic bacteria (14). Here, by establishing discrete starting coculture conditions where we initially inoculated *M. salina* with one of two bacterial strains and then subsequently facilitated recruitment of dispersed bacteria within the open, outdoor cultivation system (Fig. 1A), our study aimed to investigate whether these bacteria may additionally affect *M. salina* biomass via microbe-microbe interactions. We hypothesized that we would observe altered community assembly trajectory patterns both between our bacterially inoculated treatments and in comparison to the axenic control, potentially due to bacteria exerting priority effects and altering the subsequent establishment and assembly trajectory of the bacterial community (31, 53), resulting in divergent community composition patterns across treatments. However, our results do not fully support this hypothesis. As a whole, system-wide community composition did not vary with initial coculture inoculation treatment, as all predominant bacterial taxa were shared across mesocosms by day 17 of the experiment (cultivation round 3) (Fig. 2). There were slight differences in the estimated abundances (via relative coverage) of bacterial community members over time; for example, *Erythrobacter* sp. (MSM4) showed a lower abundance in the two initially axenic mesocosms than in the four started with the bacterial isolate strains at day 36 (see Fig. S1 in the supplemental material). This decline in *Erythrobacter* sp. was followed by a subsequent decrease in algal productivity 3 days later (Fig. 1C); however, this result is correlative, and additional variables not measured here may have also contributed to decreased algal productivity. Nevertheless, the correlation data suggest that *Erythrobacter* sp. could be a potential algal mutualist and justifies subsequent investigations of this understudied genus.

We observed cross-mesocosm dispersal of inoculated strains in addition to environmentally sourced bacteria, specifically the *Alteromonas* sp. which we detected in both control mesocosms midway through the experiment (day 17) (Table S7). In contrast, the *Phaeobacter* sp. isolate was undetectable at all time points sampled, suggesting that this bacterium failed to establish and persist. It is unclear to what extent environmental conditions and/or competitive biotic interactions influenced the establishment, abundance, and persistence of inoculated isolates and additionally how these patterns may have influenced downstream community assembly dynamics and algal-bacterial interactions. Thus, we advocate for subsequent quantitative experiments that investigate the interplay between abiotic and biotic interactions on algal-bacterial mutualisms. Interestingly, while the *Phaeobacter* isolate failed to persist, a related yet distinct *Phaeobacter* sp. (MSM14) was recruited into the mesocosms. Comparative genomics show that these are divergent strains or species, as evidenced by low nucleotide identity (89%) and distinct functional capacities. Features present in the MAG and absent from the isolate genome included protein families for siderophore and iron transport, methane monooxygenase, urea transporters and urease proteins, and vitamin B12 transporters (Table S3). The presence of methane monooxygenase genes might suggest that this organism is capable of methane metabolism and was potentially selected for in this highly reactive environment where *M. salina* may release intermediates for this process (54). In combination with complete pathways for CO oxidation and respiration (Fig. 3A), this provides compelling evidence that the *M. salina*-associated bacteria can utilize diverse single-carbon sources, and their metabolic flexibility may contribute to their enhanced survival here. The other identified functions are suggestive of a mutualistic lifestyle where bacteria

potentially influence the mobilization of iron and provide vitamins that promote algal growth. Additional phenotypic and metabolic quantification are needed to test these hypotheses in the future, for example, measuring substrate incorporation and transfer from bacteria to algal host via nanoscale stable isotope tracing (NanoSIMS) (3, 23).

Persistent bacteria capable of CO oxidation and denitrification. The low-diversity community associated with *M. salina* was numerically dominated by one taxon—a previously uncultured and undescribed member of the *Rhodobacteraceae* (MSM9; Fig. 2)—whose abundance equaled that of the other 14 MAGs combined (Table S7C). We postulate that this curated MAG is representative of one single strain, as there was no evidence of genomic variation across mesocosms or over time (9 SNPs identified out of the entire 3.76-Mb genome, or <0.001% variation). Thus, after this bacterium was recruited within at least one mesocosm, it quickly became established across the system and was retained over time, without being replaced by other closely related strains. We infer that the persistence of the *Rhodobacteraceae* species may likely be due in part to its metabolic flexibility for energy production. First, this organism, like many other members of the *Rhodobacteraceae* (55–57) including the other 4 MAGs identified within this family, is a CO oxidizer. This metabolism is hypothesized to be a physiological adaptation to enhance survival under a wide range of DOC availability (58). Second, *Rhodobacteraceae* MSM9 also has the genomic capability for denitrification, again an energy-generating process, but in this case one that could contribute to system-wide nitrogen loss to the atmosphere and potentially reduce the availability of nitrate for algae under more N-limited conditions. The fact that the most numerically dominant organism in the outdoor cultures maintains the genetic capability for two major energy-generating metabolisms suggests that the alga-associated bacteria may have been carbon limited.

Common B vitamin synthesis and anoxygenic photosynthesis in *M. salina*-associated bacteria. Second to the predominant *Rhodobacteraceae*, the 14 other recovered taxa represented a broad phylogenetic distribution (Alphaproteobacteria, Bacteroidia, Gammaproteobacteria). Six of the organisms identified at the genus level have close relatives previously identified to maintain metabolic interactions with other species of algae, including *Marinobacter* sp. (MSM2), *Algoriphagus* sp. (MSM8) (59), *Methylophaga* sp. (MSM3) (32), *Marinoscillum* sp. (MSM7) (60), *Flavobacterium* sp. (MSM5) (61), and *Phaeobacter* sp. (MSM14) (49). Four additional taxa (MSM10, MSM12, MSM13, MSM15) could not be assigned to a genus-level annotation despite the nearly complete assemblies, suggesting that neither they nor their close relatives have been cultivated previously. They share metabolic features with previously described alga-associated bacteria, which may have contributed to their recruitment here. Similar to the predominant *Rhodobacteraceae*, they display diverse carbon biogeochemical capacity, including CO oxidation potential (MSM12, MSM13) (Fig. 3; Table S3A). Two appear to be photoheterotrophs (MSM12, MSM13), which is a function shared with two other taxa (MSM4, MSM6) via conservation of the PGC gene cluster for anoxygenic photosynthesis (Table S4). The taxa which we identified as potential photoheterotrophs are all classified within the *Proteobacteria* phylum, with three classified as *Rhodobacteraceae*, an observation that is in agreement with previous studies on the evolution of photoheterotrophy in bacteria (62, 63). One of these taxa (MSM12) appears to be a denitrifying bacterium and, along with another *Rhodobacteraceae* species (MSM9) and *Marinobacter* sp. (MSM2), likely contributed to the N cycle via conversion of inorganic nitrate to atmospheric nitrogen gas, potentially promoting nitrogen loss in the system (64). We postulate that three of these four previously undescribed bacterial taxa also likely interact with *M. salina* via production of essential B vitamins, as the metabolic capacity for biosynthesis of one or more classes of B vitamins was identified, specifically, B1 (MSM10), B7 (MSM10), and B12 (MSM12, MSM13) among other taxa (all MAGs excluding MSM8, MSM9, MSM15). Algae require B vitamins and cannot biosynthesize these compounds; hence, they are dependent on an exogenous source. While the cultivation medium used in this system was replete with vitamins to encourage algal growth, these taxa may be able to maintain algal growth if vitamins become limited over time.

Community cross-feeding potential for TDA/roseobacticide synthesis. The genomic evidence from the outdoor cultures and the simple laboratory experiment together suggest that microbe-microbe interactions may influence bacterial metabolite synthesis, particularly the TDA and roseobacticide system that influences algal growth, but likely others that have not been characterized previously. Notably, the data suggest that multiple, divergent taxa could contribute distinct metabolites shown to be precursors for *P. gallaeciensis* production of algal-stimulating (TDA) or algal-senescing (roseobacticide) compounds (12, 44, 49, 65). We found it intriguing that different organisms were capable of discrete steps in this metabolic process, as toluene tolerance, PAA catabolism, and TDA production capabilities collectively have only primarily been described for two taxa (49, 65). Thus, we expected the collective process to either be conserved or lacking completely in a given genome. TDA and roseobacticide production are energetically expensive processes, and we wonder whether bacterial partitioning of the steps involved may improve community fitness via cross-feeding, a phenomenon that recent studies have shown to be prevalent in microbial community dynamics (66–68). We have proposed a community-based cooperative conceptual model (Fig. 4) that is based on our genomic observations and supported by our targeted experimental results. With increasing pCA availability, the predicted roseobacticide-producing isolate *P. gallaeciensis* BS107 reduced the growth of *M. salina* compared to axenic algae free of bacteria. However, this growth-inhibiting effect can be alleviated if pCA-degrading bacteria are added to the system. Our experiments and conceptual model suggest a cross-feeding hypothesis that pCA degraders may prevent algicidal roseobacticide production and subsequent algal growth inhibition, potentially through competition for pCA. If the roseobacticide precursor compound pCA were to become scarce due to bacterial degradation, this would instead presumably result in production by *P. gallaeciensis* of algal growth-promoting TDA compounds, since the metabolic pathway is shared but the product varies depending on availability of precursors (49). Although the pCA degrader synthetic community was predicted to be incapable of roseobacticide production from pCA, it is interesting that this consortium inhibited algal growth only when pCA was added (Fig. S2); however, the mechanism underlying the observed phenotype was not discernible based on genomic features. Since the genome-based metabolic predictions and growth assays were used as the basis for our cooperative model, we acknowledge that we lack corroborating characterizations of bacterial activity and quantification of chemical metabolites, which precludes us from assessing whether metabolites were actively being exchanged and influenced algal biomass as a result. Future investigations should combine a multi-omics (metagenomics, transcriptomics, metabolomics) approach to pinpoint the mechanisms of this proposed cooperative symbiosis.

Through the results presented here, we have begun to describe the metabolic capacity of alga-associated bacteria in high-biomass cultivation systems and to infer the community dynamics both among bacteria and with an algal partner. Given that heterotrophic bacteria tightly associate with bioenergy-relevant organisms, we expect this study to provide a framework for subsequent research to consider how ecological interactions mediate bioenergy output. These data suggest that for complex systems, ecological outcomes are difficult to predict using a reductionist approach, for example, by inoculating bioenergy crops with a single mutualist to increase output. Rather, through the experiment described here, we show that competitive interactions and metabolic complementarity must be considered, as a collective community may not behave as the sum of its parts.

MATERIALS AND METHODS

Algal and bacterial cultivation. Prior to establishment of experimental mesocosms, microalgal and bacterial strains were cultivated in the laboratory as follows. A strain of *Microchloropsis salina* (CCMP 1776) was obtained from the Provasoli-Guillard National Center for Marine Algae and Microbiota (CCMP-NCMA) at Bigelow Laboratory for Ocean Sciences (West Boothbay Harbor, MA) and was maintained in the laboratory as an axenic culture in enriched seawater medium (ESAW; pH 8.2) (69) at 21°C under constant light ($100 \mu\text{mol photons m}^{-2} \text{s}^{-1}$) and aeration. Two strains of alga-associated aquatic bacteria, *Alteromonas* sp. 110 and *Phaeobacter gallaeciensis* BS107, were acquired from the laboratory's collection of bacterial isolate stocks. Isolates were cultivated from glycerol stocks by inoculating a scraping of the

stock into 5 mL sterile marine broth liquid medium and shaken overnight at 30°C. Algal-bacterial cocultures were initiated by inoculating a 1-L axenic *M. salina* culture with 10 mL of the overnight bacterial cultures of either *P. gallaeciensis* BS107 or *Alteromonas* sp. I10, and these constituted the coculture inoculations for the subsequent experimental mesocosms.

Mesocosm experimental design. Experimental mesocosms were established 1 August 2013, cultivated in a multiround harvest, and sampled at intervals until conclusion on 10 September 2013 as follows. Mesocosms were inoculated with either (i) a coculture of *M. salina* and the bacterium *Phaeobacter gallaeciensis* BS107, (ii) a coculture of *M. salina* and the bacterium *Alteromonas* sp. I10, or (iii) an axenic culture of *M. salina* without bacteria (Fig. 1). Experimental treatments were set up in duplicate, for a total of 6 mesocosms. Mesocosms containing 16 L of ESAW medium with full F/2 nutrients (70) (see Text S1 in the supplemental material) were inoculated with *M. salina* (either in coculture with bacteria or axenic) at an initial cell density of $\sim 200,000$ algal cells mL⁻¹ and were maintained in continuous aeration via ambient air in a semicontinuous mode. Mesocosms were maintained outdoors, uncovered, and exposed to elements, and no additional temperature or lighting controls were necessary.

After initial establishment and inoculation, experimental algal-bacterial mesocosms were grown for a total duration of 40 days, with a harvesting of cells and replenishment of the culture with fresh sterile medium approximately every 8 to 9 days, when cultures presumably reached stationary phase, in order to prevent a population bottleneck. A total of 5 harvest events, in which 90% of culture was removed and 10% was retained, occurred throughout the duration of the experiment, including the final harvest at the conclusion (Fig. 1B). During each harvest cycle for all 6 mesocosms, the biomass of *M. salina* was measured using relative fluorescence units (RFU) of chlorophyll *a* and samples were collected for downstream metagenomic sequencing, modified from a previous report (33) as follows. In short, 500 mL from each mesocosm was vacuum filtered onto a 0.2- μ m Supor polyethersulfone membrane filter (Pall, Port Washington, NY), with collection of algae along with both free-living and attached bacteria. Membranes were then vortexed in 10 mL artificial seawater, washing cells off the membrane and with the intent to dislodge bacteria attached to algal cells, which was repeated twice for each membrane. The resulting 20 mL of suspension was filtered through a 1- μ m membrane filter to remove most *M. salina* cells while retaining most bacterial cells, and the filtrate was transferred to sterile 50-mL conical tubes, pelleted by centrifugation (10,000 $\times g$ for 5 min), and stored at -80°C prior to DNA extraction.

DNA extraction, library preparation, and metagenomic sequencing. Total nucleic acids were extracted and purified with a metagenomic DNA isolation kit for water (Epicentre, WI) in accordance with the manufacturer's protocol. Metagenomic libraries were constructed using the Nextera XT DNA library prep kit (Illumina, San Diego, CA) with 1 ng starting input double-stranded DNA (dsDNA). Resulting libraries with an average 250-bp insert size were paired-end sequenced (2 \times 150) on a HiSeq 2000 (Illumina, San Diego, CA) at Sandia Laboratories (Livermore, CA).

MAGs. Using bioinformatics, metagenomes were demultiplexed, filtered, and trimmed prior to assembly and annotation. Resulting high-quality sequences were collectively cross-assembled and binned into metagenome-assembled genomes (MAGs), refined, and assessed for completeness (Text S1). Bacterial MAG taxonomic annotation was assigned via phylogeny inference using GTDB-Tk v1.5.0 and the release 202 database (71, 72). Gene calls for MAGs and initial functional annotation were done with PATRIC (73). The metabolic capacity of bacterial MAGs was annotated via HMM or blastp searches against marker gene databases curated with genes and pathways pulled from KEGG (74) for C and N biogeochemical cycles (43), photoheterotrophy (62, 63), B vitamin production (9, 75), and TDA/roseobacticide production (12, 44, 65, 76). As the MAGs were not fully complete genomes, we considered a metabolic pathway to be functionally complete if $\geq 75\%$ of the genes were detected.

MAG depth and breadth of read coverage were calculated by mapping individual sample fastq files with bmap v35.85 and perfectmode=t. MAG presence/absence was determined via breadth calculations (Table S7A). The estimated abundance of each MAG was calculated using the mean of the median fold coverage (Table S7B) and was normalized by transformation to a relative proportion measurement within sample to appropriately compare MAG abundances across samples (Table S7C). The relative proportion of the mean of the median fold coverage is referred to as the "relative coverage" throughout the article for clarity.

SNP analysis was done individually for each MAG by using each of the 30 quality-processed sequencing read sets using SNIPPY v4.6 (77). Average nucleotide identity between reference isolate genomes for *Phaeobacter gallaeciensis* BS107 and *Alteromonas* sp. I10 and MAGs with similar taxonomy assignments as determined by GTDB were calculated with FastANI (78). All statistical analyses were performed in R (79) and RStudio (80) using the packages "vegan" (81) and "phyloseq" (82).

Experiments testing genome-based predictions of algal-bacterial interactions. Genome-based metabolic predictions underlying algal-bacterial interactions were tested under controlled laboratory conditions. In short, we tested the effect of the algicidal roseobacticide-producing bacterium *P. gallaeciensis* on the growth of the alga *M. salina* under the addition of the exogenous roseobacticide precursor *p*-coumaric acid (pCA) (49). To test the potential for bacterial interference of roseobacticide production via pCA degradation, a portion of the cocultures were inoculated with a laboratory-synthesized mixed community of pCA-degrading bacteria. Roseobacticide-producing *P. gallaeciensis* BS107 was available for experiments from the original mesocosm experiments; however, the mesocosm-associated bacterial genomes characterized as pCA degraders were uncultivated MAGs. As a proxy, 8 related bacterial strains previously isolated from algae (59) containing the identical and complete suite of genes for pCA degradation (44) and lacking genomic capability for roseobacticide production were used in the experiments (Text S1). Axenic *M. salina* cultures were either (i) left axenic, (ii) inoculated with *P. gallaeciensis*, (iii) inoculated with the pCA-degrading community, or (iv) inoculated with both *P. gallaeciensis* and the pCA

degraders. Cultures were grown in F/2 medium either without or with pCA (1.7 mM) (Sigma-Aldrich, St. Louis, MO) and maintained at 22°C on a 14-h-light:10-h-dark cycle. Biomass was measured daily using chlorophyll *a* relative fluorescence units on a fluorometer (Turner Designs, San Jose, CA).

Data availability. Raw sequence reads, metagenomes, and metagenome-assembled genomes are available in the NCBI Sequence Read Archive (SRA) (BioProject accession no. [PRJNA844373](https://www.ncbi.nlm.nih.gov/bioproject/PRJNA844373): *Microchloropsis salina* microbiome).

SUPPLEMENTAL MATERIAL

Supplemental material is available online only.

TEXT S1, DOCX file, 0.02 MB.

FIG S1, TIF file, 1.7 MB.

FIG S2, TIF file, 1.9 MB.

TABLE S1, XLSX file, 0.01 MB.

TABLE S2, XLSX file, 0.01 MB.

TABLE S3, XLSX file, 0.01 MB.

TABLE S4, XLSX file, 0.01 MB.

TABLE S5, XLSX file, 0.01 MB.

TABLE S6, XLSX file, 0.01 MB.

TABLE S7, XLSX file, 0.03 MB.

ACKNOWLEDGMENTS

This work was funded by LLNL Biofuels Science Focus Area grant no. SCW1039 by the Department of Energy's Genomic Sciences Program in the Office of Biological and Environmental Research. Part of this work was performed under the auspices of the U.S. Department of Energy by Lawrence Livermore National Laboratory under contract no. DE-AC52-07NA27344 (LLNL-JRNL-823856). Sandia National Laboratories is a multimission laboratory managed and operated by National Technology and Engineering Solutions of Sandia, LLC, a wholly owned subsidiary of Honeywell International, Inc., for the U.S. Department of Energy's National Nuclear Security Administration under contract DE-NA0003525.

The funders had no role in study design, data collection and interpretation, or the decision to submit the work for publication.

We thank M. S. Zatzoff for help with figure rendering, K. Rolison for assistance with lab experiments, and D. Morales for edits and thoughtful comments on the manuscript draft.

H.G., K.L.S., T.W.L., and X.M. conceived the study. H.G. conducted the experiments and collected the samples. M.B.T.-G. and E.T.Y. processed samples and performed sequencing. J.A.K. carried out the bioinformatics pipeline. M.M.M. and J.A.K. analyzed the metagenomes. M.M.M. wrote the first draft of the manuscript, and all authors contributed to revisions and approved the final manuscript.

We declare no conflicts of interest.

REFERENCES

- Cirri E, Pohnert G. 2019. Algae-bacteria interactions that balance the planktonic microbiome. *New Phytol* 223:100–106. <https://doi.org/10.1111/nph.15765>.
- Ramanan R, Kim B-H, Cho D-H, Oh H-M, Kim H-S. 2016. Algae-bacteria interactions: evolution, ecology and emerging applications. *Biotechnol Adv* 34:14–29. <https://doi.org/10.1016/j.biotechadv.2015.12.003>.
- Mayali X. 2020. NanoSIMS: microscale quantification of biogeochemical activity with large-scale impacts. *Annu Rev Mar Sci* 12:449–467. <https://doi.org/10.1146/annurev-marine-010419-010714>.
- Pomeroy LR. 1974. The ocean's food web, a changing paradigm. *Bio-science* 24:499–504. <https://doi.org/10.2307/1296885>.
- Azam F, Smith DC. 1991. Bacterial influence on the variability in the ocean's biogeochemical state: a mechanistic view, p 213–236. *In* Demers S (ed), *Particle analysis in oceanography*. Springer, Berlin, Germany.
- Azam F, Fenchel T, Field J, Gray J, Meyer-Reil L, Thingstad F. 1983. The ecological role of water-column microbes in the sea. *Mar Ecol Prog Ser* 10: 257–263. <https://doi.org/10.3354/meps010257>.
- Croft MT, Lawrence AD, Raux-Deery E, Warren MJ, Smith AG. 2005. Algae acquire vitamin B12 through a symbiotic relationship with bacteria. *Nature* 438:90–93. <https://doi.org/10.1038/nature04056>.
- Gómez-Consarnau L, Sachdeva R, Gifford SM, Cutter LS, Fuhrman JA, Sañudo-Wilhelmy SA, Moran MA. 2018. Mosaic patterns of B-vitamin synthesis and utilization in a natural marine microbial community. *Environ Microbiol* 20:2809–2823. <https://doi.org/10.1111/1462-2920.14133>.
- Sañudo-Wilhelmy SA, Gómez-Consarnau L, Suffridge C, Webb EA. 2014. The role of B vitamins in marine biogeochemistry. *Annu Rev Mar Sci* 6: 339–367. <https://doi.org/10.1146/annurev-marine-120710-100912>.
- Joint I, Tait K, Wheeler G. 2007. Cross-kingdom signalling: exploitation of bacterial quorum sensing molecules by the green seaweed *Ulva*. *Philos Trans R Soc Lond B Biol Sci* 362:1223–1233. <https://doi.org/10.1098/rstb.2007.2047>.
- Amin SA, Hmelo LR, van Tol HM, Durham BP, Carlson LT, Heal KR, Morales RL, Berthiaume CT, Parker MS, Djunaedi B, Ingalls AE, Parsek MR, Moran MA, Armbrust EV. 2015. Interaction and signalling between a

- cosmopolitan phytoplankton and associated bacteria. *Nature* 522: 98–101. <https://doi.org/10.1038/nature14488>.
12. Wang R, Gallant É, Seyedsayamdost MR. 2016. Investigation of the genetics and biochemistry of roseobacticide production in the *Roseobacter* clade bacterium *Phaeobacter inhibens*. *mBio* 7:e02118-15. <https://doi.org/10.1128/mBio.02118-15>.
 13. Morris MM, Haggerty JM, Papudeshi BN, Vega AA, Edwards MS, Dinsdale EA. 2019. Nearshore pelagic microbial community abundance affects recruitment success of giant kelp, *Macrocystis pyrifera*. *Front Microbiol* 7: 1800. <https://doi.org/10.3389/fmicb.2016.01800>.
 14. Stock W, Blommaert L, De Troch M, Manginckx S, Willems A, Vyverman W, Sabbe K. 2019. Host specificity in diatom-bacteria interactions alleviates antagonistic effects. *FEMS Microbiol Ecol* 95:fiz171. <https://doi.org/10.1093/femsec/fiz171>.
 15. Lee PA, Martinez KJL, Letcher PM, Corcoran AA, Ryan RA. 2018. A novel predatory bacterium infecting the eukaryotic alga *Nannochloropsis*. *Algal Res* 32:314–320. <https://doi.org/10.1016/j.algal.2018.04.003>.
 16. Demuez M, González-Fernández C, Ballesteros M. 2015. Algicidal microorganisms and secreted algicides: new tools to induce microalgal cell disruption. *Biotechnol Adv* 33:1615–1625. <https://doi.org/10.1016/j.biotechadv.2015.08.003>.
 17. Paul C, Pohnert G. 2011. Interactions of the algicidal bacterium *Kordia algicida* with diatoms: regulated protease excretion for specific algal lysis. *PLoS One* 6:e21032. <https://doi.org/10.1371/journal.pone.0021032>.
 18. Carney LT, Lane TW. 2014. Parasites in algae mass culture. *Front Microbiol* 5:278. <https://doi.org/10.3389/fmicb.2014.00278>.
 19. Meyer N, Bigalke A, Kaulfuß A, Pohnert G. 2017. Strategies and ecological roles of algicidal bacteria. *FEMS Microbiol Rev* 41:880–899. <https://doi.org/10.1093/femsre/fux029>.
 20. Singh A, Nigam PS, Murphy JD. 2011. Mechanism and challenges in commercialisation of algal biofuels. *Bioresour Technol* 102:26–34. <https://doi.org/10.1016/j.biortech.2010.06.057>.
 21. Davis RE, Fishman DB, Frank ED, Johnson MC, Jones SB, Kinchin CM, Skaggs RL, Venteris ER, Wigmosta MS. 2014. Integrated evaluation of cost, emissions, and resource potential for algal biofuels at the national scale. *Environ Sci Technol* 48:6035–6042. <https://doi.org/10.1021/es4055719>.
 22. Kazamia E, Aldridge DC, Smith AG. 2012. Synthetic ecology—a way forward for sustainable algal biofuel production? *J Biotechnology* 162: 163–169. <https://doi.org/10.1016/j.jbiotec.2012.03.022>.
 23. Samo TJ, Kimbrel JA, Nilson DJ, Pett-Ridge J, Weber PK, Mayali X. 2018. Attachment between heterotrophic bacteria and microalgae influences symbiotic microscale interactions. *Environ Microbiol* 20:4385–4400. <https://doi.org/10.1111/1462-2920.14357>.
 24. Shurin JB, Abbott RL, Deal MS, Kwan GT, Litchman E, McBride RC, Mandal S, Smith VH. 2013. Industrial-strength ecology: trade-offs and opportunities in algal biofuel production. *Ecol Lett* 16:1393–1404. <https://doi.org/10.1111/ele.12176>.
 25. Chaumont D. 1993. Biotechnology of algal biomass production: a review of systems for outdoor mass culture. *J Appl Phycol* 5:593–604. <https://doi.org/10.1007/BF02184638>.
 26. McBride RC, Lopez S, Meenach C, Burnett M, Lee PA, Nohilly F, Behnke C. 2014. Contamination management in low cost open algae ponds for biofuels production. *Ind Biotechnol* 10:221–227. <https://doi.org/10.1089/ind.2013.0036>.
 27. Fuhrman JA, Cram JA, Needham DM. 2015. Marine microbial community dynamics and their ecological interpretation. *Nat Rev Microbiol* 13: 133–146. <https://doi.org/10.1038/nrmicro3417>.
 28. Woese CR, Fox GE. 1977. Phylogenetic structure of the prokaryotic domain: the primary kingdoms. *Proc Natl Acad Sci U S A* 74:5088–5090. <https://doi.org/10.1073/pnas.74.11.5088>.
 29. Wilkins LGE, Ettinger CL, Jospin G, Eisen JA. 2019. Metagenome-assembled genomes provide new insight into the microbial diversity of two thermal pools in Kamchatka, Russia. *Sci Rep* 9:3059. <https://doi.org/10.1038/s41598-019-39576-6>.
 30. Dinsdale EA, Edwards RA, Hall D, Angly F, Breitbart M, Brulc JM, Furlan M, Desnues C, Haynes M, Li L, McDaniel L, Moran MA, Nelson KE, Nilsson C, Olson R, Paul J, Brito BR, Ruan Y, Swan BK, Stevens R, Valentine DL, Thurber RV, Wegley L, White BA, Rohwer F. 2008. Functional metagenomic profiling of nine biomes. *Nature* 452:629–632. <https://doi.org/10.1038/nature06810>.
 31. Nemergut DR, Schmidt SK, Fukami T, O'Neill SP, Bilinski TM, Stanish LF, Knelman JE, Darcy JL, Lynch RC, Wickey P, Ferrenberg S. 2013. Patterns and processes of microbial community assembly. *Microbiol Mol Biol Rev* 77:342–356. <https://doi.org/10.1128/MMBR.00051-12>.
 32. Kimbrel JA, Samo TJ, Ward C, Nilson D, Thelen MP, Siccardi A, Zimba P, Lane TW, Mayali X. 2019. Host selection and stochastic effects influence bacterial community assembly on the microalgal phycosphere. *Algal Res* 40:101489. <https://doi.org/10.1016/j.algal.2019.101489>.
 33. Geng H, Tran-Gyamfi MB, Lane TW, Sale KL, Yu ET. 2016. Changes in the structure of the microbial community associated with *Nannochloropsis salina* following treatments with antibiotics and bioactive compounds. *Front Microbiol* 7:1155. <https://doi.org/10.3389/fmicb.2016.01155>.
 34. Fu H, Uchimiya M, Gore J, Moran MA. 2020. Ecological drivers of bacterial community assembly in synthetic phycospheres. *Proc Natl Acad Sci U S A* 117:3656–3662. <https://doi.org/10.1073/pnas.1917265117>.
 35. Kim H, Kimbrel JA, Vaiana CA, Wollard JR, Mayali X, Buie CR. 2022. Bacterial response to spatial gradients of algal-derived nutrients in a porous microplate. *ISME J* 16:1036–1045. <https://doi.org/10.1038/s41396-021-01147-x>.
 36. Krohn-Molt I, Alawi M, Förstner KU, Wiegandt A, Burkhardt L, Indenbirken D, Thieß M, Grundhoff A, Kehr J, Tholey A, Streit WR. 2017. Insights into microalga and bacteria interactions of selected phycosphere biofilms using metagenomic, transcriptomic, and proteomic approaches. *Front Microbiol* 8:1941. <https://doi.org/10.3389/fmicb.2017.01941>.
 37. Jackrel SL, Yang JW, Schmidt KC, Deneff VJ. 2021. Host specificity of microbiome assembly and its fitness effects in phytoplankton. *ISME J* 15: 774–788. <https://doi.org/10.1038/s41396-020-00812-x>.
 38. Mönnich J, Tebben J, Bergemann J, Case R, Wohrab S, Harder T. 2020. Niche-based assembly of bacterial consortia on the diatom *Thalassiosira rotula* is stable and reproducible. *ISME J* 14:1614–1625. <https://doi.org/10.1038/s41396-020-0631-5>.
 39. Brisson V, Mayali X, Bowen B, Golini A, Thelen M, Stuart RK, Northen TR. 2021. Identification of effector metabolites using exometabolite profiling of diverse microalgae. *mSystems* 6:e00835-21. <https://doi.org/10.1128/mSystems.00835-21>.
 40. de-Bashan LE, Mayali X, Bebout BM, Weber PK, Detweiler AM, Hernandez J-P, Prufert-Bebout L, Bashan Y. 2016. Establishment of stable synthetic mutualism without co-evolution between microalgae and bacteria demonstrated by mutual transfer of metabolites (NanoSIMS isotopic imaging) and persistent physical association (fluorescent in situ hybridization). *Algal Res* 15:179–186. <https://doi.org/10.1016/j.algal.2016.02.019>.
 41. Shibl AA, Isaac A, Ochsenkühn MA, Cárdenas A, Fei C, Behringer G, Arnoux M, Drou N, Santos MP, Gunsalus KC, Voolstra CR, Amin SA. 2020. Diatom modulation of microbial consortia through use of two unique secondary metabolites. *Proc Natl Acad Sci U S A* 117:27455. <https://doi.org/10.1073/pnas.2012088117>.
 42. Teeling H, Fuchs BM, Becher D, Klockow C, Gardebrecht A, Bennis CM, Kassabgy M, Huang S, Mann AJ, Waldmann J, Weber M, Klindworth A, Otto A, Lange J, Bernhardt J, Reinsch C, Hecker M, Peplies J, Bockelmann FD, Callies U, Gerds G, Wichels A, Wiltshire KH, Glöckner FO, Schweder T, Amann R. 2012. Substrate-controlled succession of marine bacterioplankton populations induced by a phytoplankton bloom. *Science* 336: 608–611. <https://doi.org/10.1126/science.1218344>.
 43. Kieft B, Li Z, Bryson S, Crump BC, Hettich R, Pan C, Mayali X, Mueller RS. 2018. Microbial community structure–function relationships in Yaquina Bay Estuary reveal spatially distinct carbon and nitrogen cycling capacities. *Front Microbiol* 9:1282. <https://doi.org/10.3389/fmicb.2018.01282>.
 44. Calero P, Jensen SI, Bojanović K, Lennen RM, Koza A, Nielsen AT. 2018. Genome-wide identification of tolerance mechanisms toward *p*-coumaric acid in *Pseudomonas putida*. *Biotechnol Bioeng* 115:762–774. <https://doi.org/10.1002/bit.26495>.
 45. Calero P, Jensen SI, Nielsen AT. 2016. Broad-host-range ProUSER vectors enable fast characterization of inducible promoters and optimization of *p*-coumaric acid production in *Pseudomonas putida* KT2440. *ACS Synth Biol* 5:741–753. <https://doi.org/10.1021/acssynbio.6b00081>.
 46. Berger M, Brock NL, Liesegang H, Dogs M, Preuth I, Simon M, Dickschat JS, Brinkhoff T. 2012. Genetic analysis of the upper phenylacetate catabolic pathway in the production of tropodithietic acid by *Phaeobacter gallaeciensis*. *Appl Environ Microbiol* 78:3539–3551. <https://doi.org/10.1128/AEM.07657-11>.
 47. Duan Y, Petzold M, Saleem-Batcha R, Teufel R. 2020. Bacterial tropone natural products and derivatives: overview of their biosynthesis, bioactivities, ecological role and biotechnological potential. *Chembiochem* 21: 2384–2407. <https://doi.org/10.1002/cbic.201900786>.
 48. Wilson MZ, Wang R, Gitai Z, Seyedsayamdost MR. 2016. Mode of action and resistance studies unveil new roles for tropodithietic acid as an anti-cancer agent and the γ -glutamyl cycle as a proton sink. *Proc Natl Acad Sci U S A* 113:1630–1635. <https://doi.org/10.1073/pnas.1518034113>.

49. Seyedsayamdost MR, Case RJ, Kolter R, Clardy J. 2011. The Jekyll-and-Hyde chemistry of *Phaeobacter gallaeciensis*. *Nat Chem* 3:331–335. <https://doi.org/10.1038/nchem.1002>.
50. Frank O, Pradella S, Rohde M, Scheuner C, Klenk H-P, Göker M, Petersen J. 2014. Complete genome sequence of the *Phaeobacter gallaeciensis* type strain CIP 105210 T (= DSM 26640 T = BS107 T). *Stand Genomic Sci* 9: 914–932. <https://doi.org/10.4056/signs.5179110>.
51. Lutz GA, Turgut Dunford N. 2018. Interactions of microalgae and other microorganisms for enhanced production of high-value compounds. *Front Biosci (Landmark Ed)* 23:1487–1504. <https://doi.org/10.2741/4656>.
52. Le Chevanton M, Garnier M, Lukomska E, Schreiber N, Cadoret J-P, Saint-Jean B, Bougaran G. 2016. Effects of nitrogen limitation on *Dunaliella* sp. -*Alteromonas* sp. interactions: from mutualistic to competitive relationships. *Front Mar Sci* 3:123.
53. Fukami T. 2015. Historical contingency in community assembly: integrating niches, species pools, and priority effects. *Annu Rev Ecol Syst* 46: 1–23. <https://doi.org/10.1146/annurev-ecolsys-110411-160340>.
54. Ernst L, Steinfeld B, Barayeu U, Klintzsch T, Kurth M, Grimm D, Dick TP, Rebelein JG, Bischofs IB, Keppler F. 2022. Methane formation driven by reactive oxygen species across all living organisms. *Nature* 603:482–487. <https://doi.org/10.1038/s41586-022-04511-9>.
55. Tolli JD, Sievert SM, Taylor CD. 2006. Unexpected diversity of bacteria capable of carbon monoxide oxidation in a coastal marine environment, and contribution of the *Roseobacter*-associated clade to total CO oxidation. *Appl Environ Microbiol* 72:1966–1973. <https://doi.org/10.1128/AEM.72.3.1966-1973.2006>.
56. Moran MA, Miller WL. 2007. Resourceful heterotrophs make the most of light in the coastal ocean. *Nat Rev Microbiol* 5:792–800. <https://doi.org/10.1038/nrmicro1746>.
57. Cunliffe M. 2011. Correlating carbon monoxide oxidation with *cox* genes in the abundant marine *Roseobacter* clade. *ISME J* 5:685–691. <https://doi.org/10.1038/ismej.2010.170>.
58. Cordero PRF, Bayly K, Man Leung P, Huang C, Islam ZF, Schittenhelm RB, King GM, Greening C. 2019. Atmospheric carbon monoxide oxidation is a widespread mechanism supporting microbial survival. *ISME J* 13: 2868–2881. <https://doi.org/10.1038/s41396-019-0479-8>.
59. Chorazyczewski AM, Huang I-S, Abdulla H, Mayali X, Zimba PV. 2021. The influence of bacteria on the growth, lipid production, and extracellular metabolite accumulation by *Phaeodactylum tricornutum* (Bacillariophyceae). *J Phycol* 57:931–940. <https://doi.org/10.1111/jpy.13132>.
60. Karimi E, Geslain E, KleinJan H, Tanguy G, Legeay E, Corre E, Dittami SM. 2020. Genome sequences of 72 bacterial strains isolated from *Ectocarpus subulatus*: a resource for algal microbiology. *Genome Biol Evol* 12: 3647–3655. <https://doi.org/10.1093/gbe/evz278>.
61. Mayali X, Doucette GJ. 2002. Microbial community interactions and population dynamics of an algicidal bacterium active against *Karenia brevis* (Dinophyceae). *Harmful Algae* 1:277–293. [https://doi.org/10.1016/S1568-9883\(02\)00032-X](https://doi.org/10.1016/S1568-9883(02)00032-X).
62. Bill N, Tomasch J, Riemer A, Müller K, Kleist S, Schmidt-Hohagen K, Wagner-Döbler I, Schomburg D. 2017. Fixation of CO₂ using the ethylmalonyl-CoA pathway in the photoheterotrophic marine bacterium *Dinoroseobacter shibae*: CO₂ fixation in *Dinoroseobacter shibae*. *Environ Microbiol* 19:2645–2660. <https://doi.org/10.1111/1462-2920.13746>.
63. Brinkmann H, Göker M, Koblížek M, Wagner-Döbler I, Petersen J. 2018. Horizontal operon transfer, plasmids, and the evolution of photosynthesis in Rhodobacteraceae. *ISME J* 12:1994–2010. <https://doi.org/10.1038/s41396-018-0150-9>.
64. Liu Y, Ai G-M, Miao L-L, Liu Z-P. 2016. *Marinobacter* strain NNA5, a newly isolated and highly efficient aerobic denitrifier with zero N₂O emission. *Bioreour Technol* 206:9–15. <https://doi.org/10.1016/j.biortech.2016.01.066>.
65. Brock NL, Nikolay A, Dickschat J. 2014. Biosynthesis of the antibiotic tropodithietic acid by the marine bacterium *Phaeobacter inhibens*. *Chem Commun (Camb)* 50:5487–5489. <https://doi.org/10.1039/c4cc01924e>.
66. Seth EC, Taga ME. 2014. Nutrient cross-feeding in the microbial world. *Front Microbiol* 5:350. <https://doi.org/10.3389/fmicb.2014.00350>.
67. Sokolovskaya OM, Shelton AN, Taga ME. 2020. Sharing vitamins: cobamides unveil microbial interactions. *Science* 369:eaba0165. <https://doi.org/10.1126/science.aba0165>.
68. D'Souza G, Shitut S, Preussger D, Yousif G, Waschina S, Kost C. 2018. Ecology and evolution of metabolic cross-feeding interactions in bacteria. *Nat Prod Rep* 35:455–488. <https://doi.org/10.1039/c8np00009c>.
69. Harrison PJ, Waters RE, Taylor FJR. 1980. A broad spectrum artificial sea water medium for coastal and open ocean phytoplankton. *J Phycol* 16: 28–35. <https://doi.org/10.1111/j.1529-8817.1980.tb00724.x>.
70. Guillard RRL, Ryther JH. 1962. Studies of marine planktonic diatoms. I. *Cyclotella nana* Hustedt and *Detonula confervacea* Cleve. *Can J Microbiol* 8:229–239. <https://doi.org/10.1139/m62-029>.
71. Parks DH, Chuvochina M, Waite DW, Rinke C, Skarshewski A, Chaumeil P-A, Hugenholtz P. 2018. A standardized bacterial taxonomy based on genome phylogeny substantially revises the tree of life. *Nat Biotechnol* 36:996–1004. <https://doi.org/10.1038/nbt.4229>.
72. Parks DH, Chuvochina M, Chaumeil P-A, Rinke C, Mussig AJ, Hugenholtz P. 2020. A complete domain-to-species taxonomy for Bacteria and Archaea. *Nat Biotechnol* 38:1079–1086. <https://doi.org/10.1038/s41587-020-0501-8>.
73. Brettin T, Davis JJ, Disz T, Edwards RA, Gerdes S, Olsen GJ, Olson R, Overbeek R, Parrello B, Pusch GD, Shukla M, Thomason JA, Stevens R, Vonstein V, Wattam AR, Xia F. 2015. RASTtk: a modular and extensible implementation of the RAST algorithm for building custom annotation pipelines and annotating batches of genomes. *Sci Rep* 5:8365. <https://doi.org/10.1038/srep08365>.
74. Kanehisa M, Goto S. 2000. KEGG: kyoto encyclopedia of genes and genomes. *Nucleic Acids Res* 28:27–30. <https://doi.org/10.1093/nar/28.1.27>.
75. Doxey AC, Kurtz DA, Lynch MD, Sauder LA, Neufeld JD. 2015. Aquatic metagenomes implicate Thaumarchaeota in global cobalamin production. *ISME J* 9:461–471. <https://doi.org/10.1038/ismej.2014.142>.
76. Sonnenschein EC, Phippen CBW, Bentzon-Tilia M, Rasmussen SA, Nielsen KF, Gram L. 2018. Phylogenetic distribution of roseobactin in the *Roseobacter* group and their effect on microalgae: distribution of roseobactin and their effect. *Environ Microbiol Rep* 10:383–393. <https://doi.org/10.1111/1758-2229.12649>.
77. Seemann T. 2015. snippy: fast bacterial variant calling from NGS reads. <https://github.com/tseemann/snippy>.
78. Jain C, Rodriguez-R LM, Phillippy AM, Konstantinidis KT, Aluru S. 2018. High throughput ANI analysis of 90K prokaryotic genomes reveals clear species boundaries. *Nat Commun* 9:5114. <https://doi.org/10.1038/s41467-018-07641-9>.
79. R Core Team. 2021. R: a language and environment for statistical computing. R Foundation for Statistical Computing, Vienna, Austria. <https://www.R-project.org/>.
80. RStudio Team. 2021. RStudio: integrated development environment for R. RStudio, PBC, Boston, MA. <http://www.rstudio.com/>.
81. McGlenn D, Oksanen J, Guillaume Blanchet F, Friendly M, Kindt R, Legendre P, Minchin PR, O'Hara RB, Simpson GL, Solymos P, Stevens MHH, Szoecs E, Wagner H. 2020. vegan: community ecology package (R package version 2.5–7). <https://CRAN.R-project.org/package=vegan>.
82. McMurdie PJ, Holmes S. 2013. phyloseq: an R package for reproducible interactive analysis and graphics of microbiome census data. *PLoS One* 8: e61217. <https://doi.org/10.1371/journal.pone.0061217>.